Measurement of the OH Reaction Rate Constants for CF_3CH_2OH, $CF_3CF_2CH_2OH$, and $CF_3CH(OH)CF_3$

Kazuaki Tokuhashi,*,† Hidekazu Nagai,† Akifumi Takahashi,† Masahiro Kaise,† Shigeo Kondo,† Akira Sekiya,† Mitsuru Takahashi,‡ Yoshihiko Gotoh,† and Atsuo Suga‡

National Institute of Materials and Chemical Research, 1-1 Higashi, Tsukuba, Ibaraki 305, Japan, and Research Institute of Innovative Technology for the Earth, Hongo Wakai Building, 2-40-17, Hongo, Bunkyo-ku, Tokyo 113, Japan

Received: October 5, 1998; In Final Form: December 30, 1998

The OH reaction rate constants have been measured for CF_3CH_2OH, $CF_3CF_2CH_2OH$, and $CF_3CH(OH)CF_3$ over the temperature range 250−430K. Kinetic measurements have been carried out using the discharge flow, laser photolysis, and flash photolysis methods, combined respectively with the laser-induced fluorescence technique to monitor the OH radical concentrations. The influence of impurities contained in the sample of $CF_3CF_2CH_2OH$ has been investigated by means of sample purification using gas chromatography. No sizable effect of impurities was found on the measured rate constants of these three fluorinated alcohols. The Arrhenius rate constants have been determined from the respective kinetic data as $k(CF_3CH_2OH) = (2.00 \pm 0.37) \times 10^{-12} \exp[-(890 \pm 60)/T]$, $k(CF_3CF_2CH_2OH) = (1.40 \pm 0.27) \times 10^{-12} \exp[-(780 \pm 60)/T]$, and $k(CF_3CH(OH)CF_3) = (6.99 \pm 1.56) \times 10^{-13} \exp[-(990 \pm 70)/T]$ cm^3 molecule^{-1} s^{-1}. A method of predicting the OH reaction rate constants for fluorinated alcohols, hydrofluorocarbons, alkanes, and alcohols has been proposed.

Introduction

Fully halogenated chlorofluorocarbons (CFCs) cause depletion of the stratospheric ozone layer as well as global warming. Partially fluorinated alcohols are important in relevance with potential substitutes of CFCs. Since, these molecules do not contain Cl atoms, they do not contribute to the ozone depletion, but may potentially cause the global warming effect. In general, the molecules of these substances contain hydrogen atoms, and are expected to be oxidized by OH radicals in the atmosphere.[1] Therefore, study of the reactivity against OH radicals is indispensable for the evaluation of atmospheric lifetime of these molecules. Although there are numerous data of rate constants for various compounds, there is little information regarding the OH reaction rate constants for fluorinated alcohols. In this paper, we report the results of the kinetic measurements for the reactions of OH radicals with CF_3CH_2OH, $CF_3CF_2CH_2OH$, and $CF_3CH(OH)CF_3$ over the temperature range 250−430 K. Effects of impurities on the measured rate constants have been investigated by the sample purification with gas chromatography. On the other hand, to obtain the reaction kinetic data from the experiment, considerable labor is required. It is desirable to develop the empirical prediction method of the reaction rate constants. In this paper, we have reexamined the prediction method of OH reaction rate constants which considers the contributions from the substituent groups. The prediction method is applicable to the OH reaction rate constants of fluorinated alcohols, hydrofluorocarbons, alkanes, and alcohols.

Experimental Section

The OH reaction rate constants have been measured for CF_3CH_2OH, $CF_3CF_2CH_2OH$, and $CF_3CH(OH)CF_3$ over the temperature range 250−430 K by the discharge flow (DF), laser photolysis (LP), and flash photolysis (FP) techniques. In all cases, the experiments have been carried out under a large excess of reactant (fluorinated alcohols) over the initial OH radical concentrations. The concentration of OH radicals has been measured by the laser-induced fluorescence (LIF) method.

Discharge Flow (DF) Method. The schematic diagram of the discharge flow reactor is shown in Figure 1. Two flow tubes about 700 and 900 mm long were used in the kinetic study. They are made of Pyrex glass and are 20 mm in inner diameter. The flow tubes are accommodated with a movable double sliding injector[2] made of stainless steel. Helium was used as the primary carrier gas. OH radicals are produced by the reaction

$$H + NO_2 \rightarrow OH + NO$$

where hydrogen atoms are generated by microwave discharge of Ar gas containing a trace amount of hydrogen. NO_2 diluted with Ar is supplied in excess to the flow tube through the top of the outer tube (6 mm o.d.) of the sliding injector. The reactant vapor is added to the gas stream through the top of the inner tube (3 mm o.d.) of the sliding injector. The top of the inner tube is located 400 mm (for 700 mm tube) or 500 mm (for 900 mm tube) downstream from the top of the outer tube. Both the flow tube and the sliding injector are coated with Teflon to minimize wall loss of OH radicals. To establish a stable profile of the reactant concentration in a short time, helium gas is always slowly supplied to the inner tube of the sliding injector together with the reactant vapor. The position of the sliding injector was controlled by a pulse stage connected with a pulse controller. A typical experimental condition is as follows: total pressure is 4−6 Torr, the linear flow velocity of gas mixture is 5−14 m s^{-1}, and the NO_2 concentration is (1.7−14) × 10^{13} molecule cm^{-3}. Initial concentration of OH radicals, which is a function of the hydrogen flow rate, is (0.2−

* Author to whom correspondence should be addressed at Department of Physical Chemistry, National Institute of Materials and Chemical Research, 1-1 Higashi, Tsukuba, Ibaraki 305, Japan.
† National Institute of Materials and Chemical Research.
‡ Research Institute of Innovative Technology for the Earth.

10.1021/jp983961x CCC: $18.00
Published on Web 03/19/1999

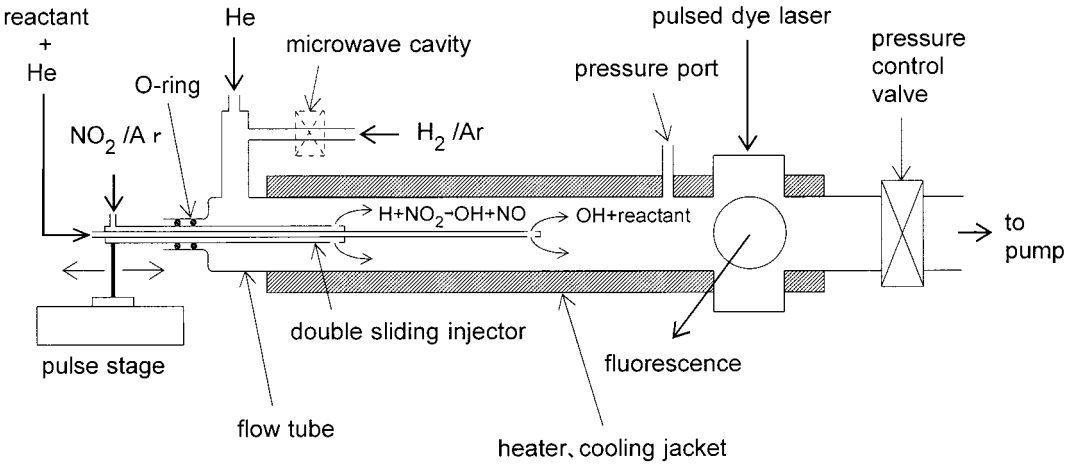

Figure 1. Schematic diagram of the discharge flow reactor.

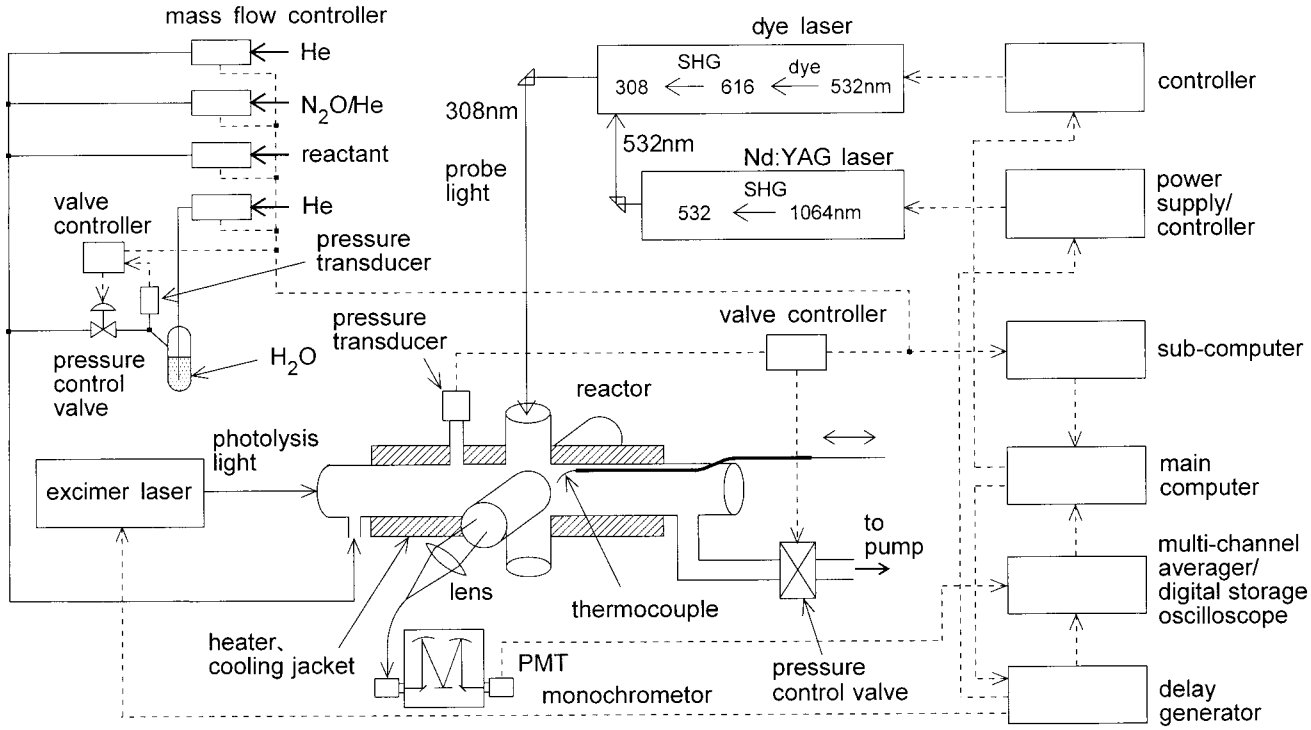

Figure 2. Schematic diagram of the laser photolysis/laser-induced fluorescence apparatus.

1.0) $\times$ 10^{11} molecule cm^{-3}. The primary carrier gas, He (99.995%), was purified by heated copper oxide followed by a liquid nitrogen trap. H_2 diluted with a large excess of Ar was prepared manometrically in a stainless steel vessel, or purchased as a mixture with a H_2 concentration of around 0.005%. The samples of H_2 (99.99%) and Ar (99.995%) were used without further purification. NO_2 (99.5% up) diluted with Ar was purchased as a mixture with an NO_2 concentration of 1−2%.

Laser Photolysis (LP) and Flash Photolysis (FP) Methods. A schematic diagram of the LP-LIF apparatus is shown in Figure 2. The Pyrex glass reactor with inner diameter of 25 mm is used for the LP and FP experiments. The length of the reactor is 40 cm. In the case of LP method, OH radicals are produced by the reaction

$$O(^1D) + H_2O \rightarrow 2OH$$

where $O(^1D)$ atoms are generated by photodissociation of N_2O with an ArF excimer laser (Japan Storage Battery, EXL-200) in the presence of He bath gas at a total pressure of 15−70 Torr. The power density of the excimer laser at the exit window of the reaction cell is around 2−5 mJ cm^{-2} $pulse^{-1}$. To ensure rapid conversion of $O(^1D)$ atoms to OH radicals, the ratio of H_2O to N_2O is kept larger than about 20:1. N_2O concentration is about (1.2−4.0) $\times$ 10^{14} molecule cm^{-3}. The photolyzing light is directed to the reaction cell along the axial line of the cell through a quartz window.

The apparatus used in the FP method is almost the same as that for the LP method shown in Figure 2 except for the photolysis light source and the gases used. In the case of the FP method, H_2O (100−200 mTorr) is directly photolyzed with pulsed light of Xe flash lamp (EG & G, FX-193U, 600-1300 V and 2 μF, 0.36−1.69 J $pulse^{-1}$, typically 0.64 J $pulse^{-1}$, pulse width is 10−20 μs, $\lambda \geq 180$ nm, quartz cutoff). The photolyzing light is weakly focused by quartz lenses, and is directed to the reaction cell along the axial line through the quartz window. Ar is used as carrier gas in most cases (some experiments have

been carried out using a He carrier). The region between the flash lamp (or excimer laser for the LP method) and the reaction cell is purged with dry N_2.

Water vapor was supplied by bubbling a certain part of carrier gas through a vessel filled with water at room temperature. The total pressure of carrier gas containing water vapor was measured by a capacitance manometer, and was kept constant by a control valve. The amount of water vapor supplied to the reaction cell was estimated from the flow rate of the carrier gas, water temperature measured by CA thermocouple (type K), and total pressure of carrier gas containing water vapor. To prevent accumulation of photofragments or reaction products in the cell, all photolysis experiments were carried out under slow flow conditions. For both LP and FP methods, initial concentration of OH radicals, which is estimated from comparison with fluorescence intensities obtained with the DF method, is always kept smaller than 10^{11} molecule cm^{-3}. The repetition rate of the photolysis light was set as 10 Hz.

A primary carrier gas, He (99.995%) or Ar (99.995%) was used without further purification. N_2O (99.999%) diluted with He was purchased as a mixture with N_2O concentration of around 1%.

Laser-Induced Fluorescence Method. The concentration of OH radicals has been measured by the LIF method. In the case of DF and FP methods, the apparatus is the same as that for the LP method shown in Figure 2. The excitation light is from a frequency-doubled tunable dye laser (Spectron, SL4000B), and the wavelength was tuned at about 308 nm. The dye laser was pumped by pulsed light of a frequency-doubled Nd:YAG laser (Spectron, SL803). The repetition rate of the laser was set as 10 Hz. Fluorescence signals due to OH radicals were monitored at a right angle against both the excitation light and the photolysis light (or flow tube for the DF method), and focused by quartz lenses and a concave mirror, and detected by a photomultiplier tube. The scattered light of the excitation light (and photolysis light source for LP and FP methods) was reduced by a monochromator (Jarrell−Ash, Monospec 25, 2360G/mm, 25 cm focal length). The output signal of the photomultiplier tube was amplified by a preamplifier, and accumulated (usually 400−600 shots) by a multichannel scaler/averager (Stanford, SR430), or averaged (usually 128 shots by a digital storage oscilloscope Gould-4050), and stored in a microcomputer for further data processing. Trigger pulses for YAG laser, multichannel scaler/averager (or digital storage oscilloscope), and photolysis light source were generated by a delay generator (Stanford, DG535). This computer was used to control the delay generator (for LP and FP methods), pulse controller (to determine the position of sliding injector for DF method), and the other computer (see later).

Gas Handling and Measurements. Various gas flow rates were measured and controlled by calibrated mass flow controllers. In particular, the flow rate of fluorinated alcohol vapor was directly measured and controlled by the calibrated mass flow controller. For gaseous materials, calibration of the mass flow controllers was made with a gas meter or a soap-film flow meter. For liquid materials (fluorinated alcohols), calibration of the mass flow controller was made by measuring the time−pressure relationship in the vessel with a known volume using a capacitance manometer, during which the sample vapor was supplied to the evacuated vessel through the mass flow controller. The total gas pressure of the reactor was monitored by using a capacitance manometer (MKS Baratron), and was kept constant by an electrically controlled exhaust throttle valve located downstream of the reactor. The temperature of the reactor was maintained either by electric heater (298−430 K), or by circulating heated water (298−339 K) and cooled ethanol−water mixture (250−273 K) in the outer jacket of the reaction cell from a thermostated bath. It was measured by CA thermocouple at the top of the inner tube of the sliding injector (for the DF method) or at the spot around 1−2 cm downstream from the probe laser beam (for LP and FP methods). During the experiments, the temperature across the reaction volume was maintained better than ±2 K over the temperature range examined. The gas flow rates, the total pressure, and the reaction temperature were monitored by the second computer through a digital recorder or data acquisition controller, and stored in a computer via RS-232C circuit. To ensure that the experimental data are free from any systematic errors, the experiments were repeated at intervals from several days to several months under a variety of flow conditions.

Sample Analysis and Purification. The samples of fluorinated alcohols were analyzed by using gas chromatography with an FID detector, where the area ratio of main peak against total area was taken as the purity of the sample. The analytical columns used in the present work are G-205 (1.2 mm i.d., 40 m long, film thickness 5 μm, Chemicals Inspection & Testing Institute, Japan, He carrier gas), or stainless steel column (3 mm i.d., 10 m long) packed with mainly Silicone DC 702 (Shimadzu, N_2 carrier gas). The lower value obtained using two columns was taken as a purity of the sample. The purities of CF_3CH_2OH and $CF_3CH(OH)CF_3$ samples were found to be 99.994 and 99.999%, respectively, and these samples were used without further purification. The sample of $CF_3CF_2CH_2OH$ (99.56%) was purified by gas chromatography. In the purification process, the vapor of $CF_3CF_2CH_2OH$ was charged in an evacuated sampling tube (inner volume of about 50 cm^3), and supplied to a stainless steel column (9.6 mm i.d., 4 m long) packed with Silicone DC 702 through a six-way switching cock. Nitrogen was used as the carrier gas. The middle fraction of the main peak (chromatogram was always monitored by TCD detector) was collected through a four-way switching cock into a trap cooled with liquid nitrogen. The sample of $CF_3CF_2CH_2OH$ thus obtained showed purity of 99.935%.

Results and Discussion

According to the gas chromatographic analysis made before the kinetic measurement, the purities of the samples of fluorinated alcohols as supplied are 99.994, 99.56, and 99.999% for CF_3CH_2OH, $CF_3CF_2CH_2OH$, and $CF_3CH(OH)CF_3$, respectively. The individual impurities were not characterized though. At any rate, since the impurity levels of CF_3CH_2OH and $CF_3CH(OH)CF_3$ in particular are extremely low, it is obvious that the effects of impurities on the measurement of the OH rate constants may be negligibly small for these samples. We began with measuring the OH reaction rate constant for CF_3CH_2OH and $CF_3CH(OH)CF_3$.

Figure 3 shows a typical example of a pseudo-first-order OH decay plot obtained with the DF method for various CF_3CH_2OH concentrations. Since these plots show a linear relationship, the pseudo-first-order rate constant (k_{obs}) can be derived from the slopes of the straight lines by least-squares fit to each decay plot. In Figure 4, the observed pseudo-first-order rate constants are plotted against CF_3CH_2OH concentration. In the case of the DF method, a small correction factor (usually 1 to 3%) is applied to each pseudo-first-order rate constants to account for the axial diffusion effects.[3] The plotted points are distributed along a straight line, and the bimolecular rate constant for the reaction of OH with CF_3CH_2OH can be derived from the slope by the

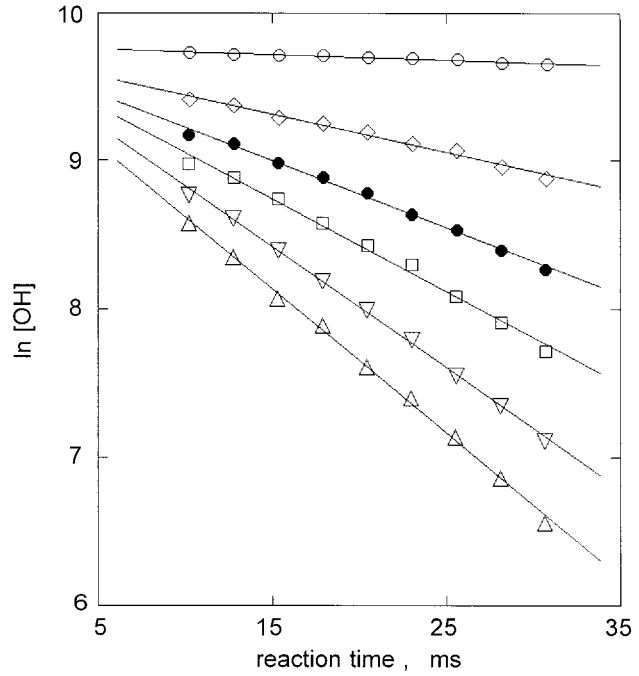

Figure 3. Pseudo-first-order decay of OH for various CF_3CH_2OH concentrations. DF-LIF method. $P = 5$ Torr, $U = 9.8$ m s^{-1}, $T = 298$ K. [CF_3CH_2OH]/10^{14} molecule cm^{-3}; (○), 0; (◇), 2.39; (●), 3.93; (□), 5.51; (▽), 7.08; (△), 8.65.

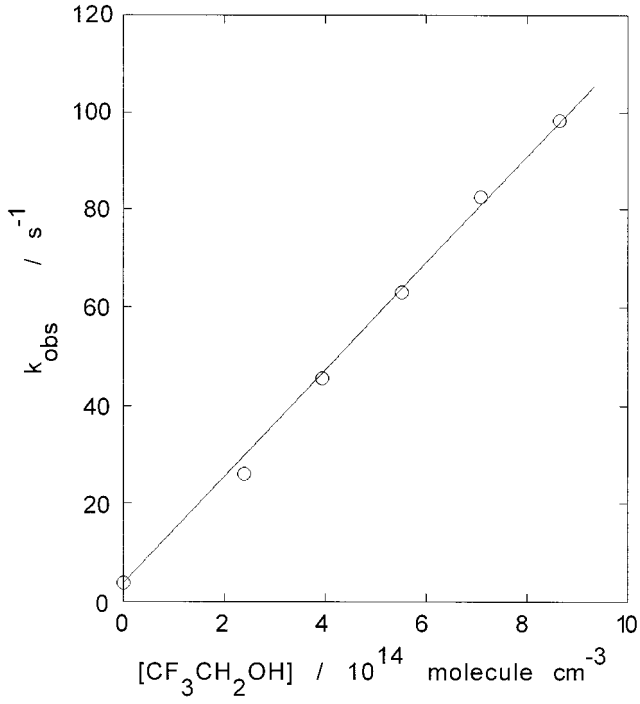

Figure 4. Plot of the observed pseudo-first-order rate constant k_{obs} against the CF_3CH_2OH concentration. DF-LIF method. $P = 5$ Torr, $U = 9.8$ m s^{-1}, $T = 298$ K.

linear least-squares fit to the observed data. The small intercept observed when there is no reactant (k_w) is attributable to the wall loss of OH radicals and also to a gas-phase reaction as

$$OH + NO_2 + M \rightarrow HNO_3 + M$$

Hence, the intercept depends on the experimental conditions. To ensure that there are no systematic errors, the experiments were repeated at intervals ranging from several days to a few months under a variety of experimental conditions including

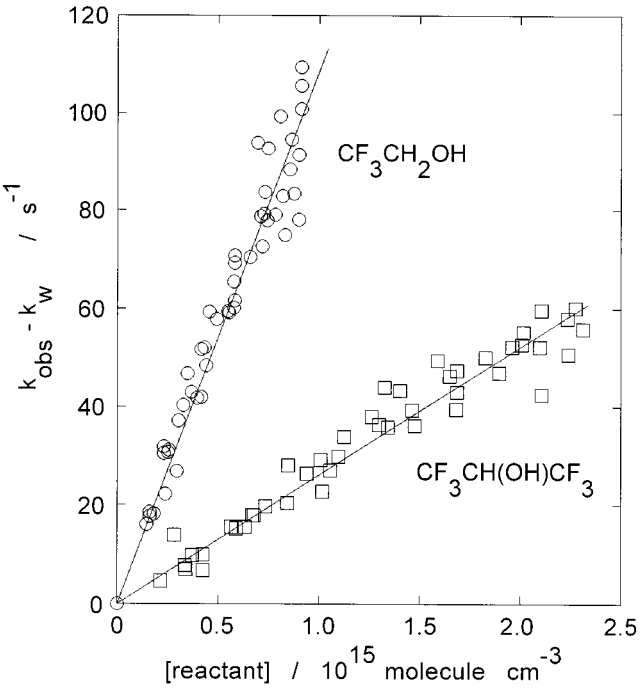

Figure 5. Plot of the pseudo-first-order rate constants corrected for wall loss, $k_{obs} - k_w$, against (○) CF_3CH_2OH, and (□) $CF_3CH(OH)CF_3$ concentrations at 298 K. DF-LIF method.

NO_2 and H_2 concentrations, linear flow velocity of the gas, and the total pressure. Figure 5 summarizes the observed data of ($k_{obs} - k_w$) for CF_3CH_2OH and $CF_3CH(OH)CF_3$ plotted against concentrations. From each set of the plot of k_{obs} versus reactant concentration, the background value (k_w) is subtracted, and the results are shown in Figure 5 as functions of CF_3CH_2OH and $CF_3CH(OH)CF_3$ concentrations. Both plots give linear relationships with relatively small scatters. Thus, it is concluded that the present rate constants derived from the least-squares fits are not affected by any of the experimental factors such as total pressure, linear velocity of gas, or H_2 and NO_2 concentrations.

Figure 6 shows a typical example of a pseudo-first-order OH decay plot obtained with the LP method for various CF_3CH_2-OH concentrations. In Figure 7, the observed pseudo-first-order rate constants, which are derived from the slopes of the straight lines by least-squares fit to each decay plot, are plotted against CF_3CH_2OH concentration. In the case of FP method, both of the pseudo-first-order plots and the k_{obs} versus reactant concentration plots give linear relationships similar to the ones for the DF and LP methods shown in Figures 3, 4, 6, and 7. In the case of LP and FP methods, the intercept of k_{obs} versus reactant concentration for zero reactant (k_d) is attributed to the diffusion of OH radicals from the viewing zone, and is partially caused by the reaction of OH with impurities contained in the gas mixture. The k_d was again dependent on the experimental conditions. For each set, the value of k_d was subtracted from k_{obs} to plot the latter against reactant concentrations. Figure 8 summarizes the example of observed data of ($k_{obs} - k_d$) for CF_3CH_2OH and $CF_3CH(OH)CF_3$ plotted against concentrations obtained with LP method. The plots of $k_{obs} - k_d$ versus reactant concentration give a linear relationship, where the scatter of the data points is about the same as in the case of the DF method shown in Figure 5. In the case of the FP method, the linearity and the scatter of the plots of $k_{obs} - k_d$ versus reactant concentration is similar to the ones for the DF and LP methods shown in Fiures 5 and 8. Thus, it can be said that the rate constants obtained for the LP and FP methods are free from

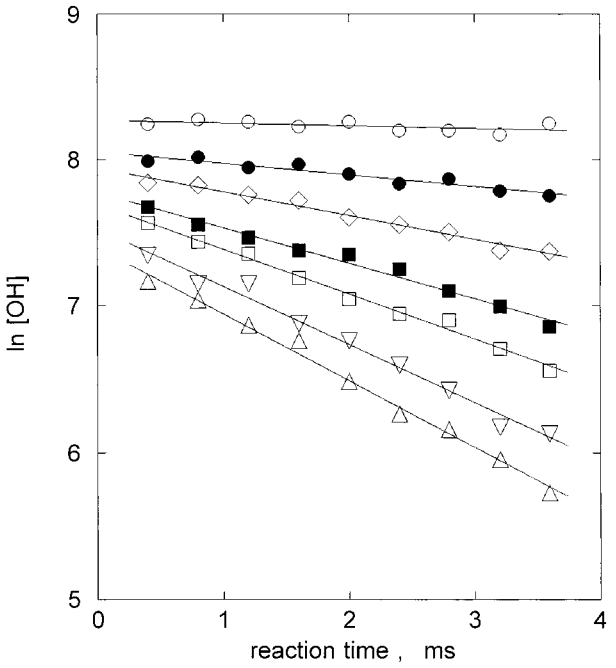

Figure 6. Pseudo-first-order decay of OH for various CF_3CH_2OH concentrations. LP-LIF method. $P = 40$ Torr, $T = 298$ K. [CF_3CH_2OH]/10^{15} molecule cm^{-3}; (○), 0; (●), 0.78; (◇), 1.55; (■), 2.39; (□), 3.15; (▽), 4.00; (△), 4.74.

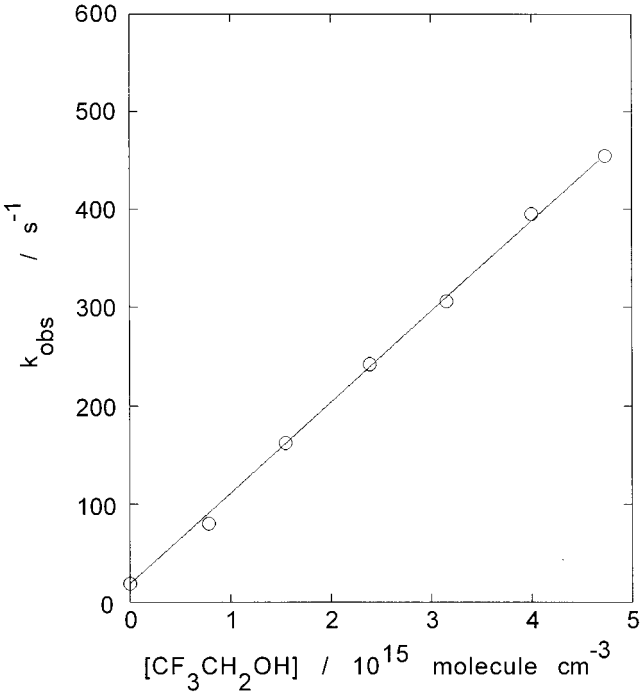

Figure 7. Plot of the observed pseudo-first-order rate constant k_{obs} against CF_3CH_2OH concentration. LP-LIF method. $P = 40$ Torr, $T = 298$ K.

the daily fluctuation of experimental conditions such as the total pressure, residence time of gas mixture, H_2O and N_2O concentrations, laser power, and discharge energy of the Xe flash lamp, at the ordinary experimental conditions.

Table 1 summarizes the OH reaction rate constants for CF_3CH_2OH and $CF_3CH(OH)CF_3$ at room temperature (298 K) obtained by using DF, LP, and FP methods. Here, the error limits of our results are at the 95% confidence level derived from the linear least-squares fit to the plot of first-order rate constant versus reactant concentration, and the systematic errors

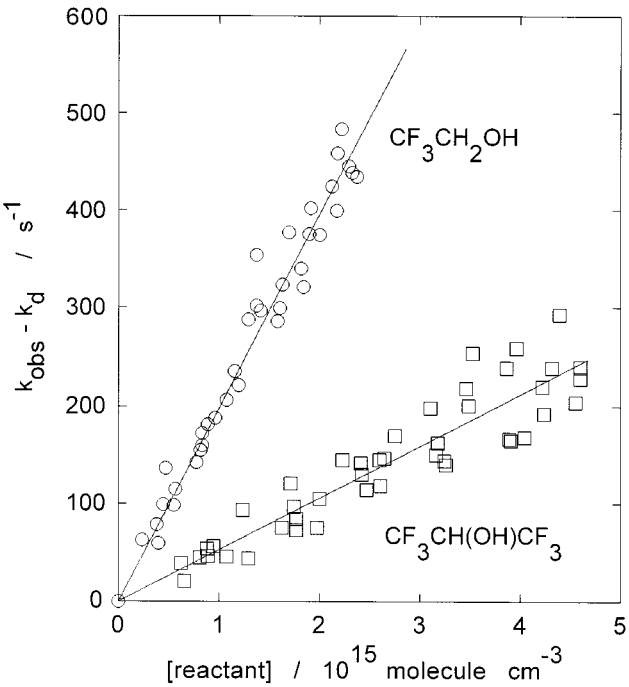

Figure 8. Plot of the pseudo-first-order rate constants corrected for wall loss, $k_{obs} - k_d$, against (○) CF_3CH_2OH, and (□) $CF_3CH(OH)CF_3$ concentrations at 298 K. LP-LIF method.

TABLE 1: Rate Constants for the Reactions of OH Radicals with Fluorinated Alcohols at Room Temperature

fluorinated alcohol	$k \times 10^{14}$ (cm^3 $molecule^{-1}$ s^{-1})	technique[a]	reference[b]
CF_3CH_2OH	10.7 ± 0.5	DF-LIF	this work
	9.86 ± 0.41	LP-LIF	this work
	9.68 ± 0.23	FP-LIF	this work
	9.55 ± 0.71	FP−RF	[4]
	9.44 ± 0.96	LP-LIF	[5]
$CF_3CF_2CH_2OH$	10.5 ± 0.5	DF-LIF	this work
	9.78 ± 0.37	LP-LIF	this work
	9.74 ± 0.35	FP-LIF	this work
	8.66 ± 0.68	LP-LIF	[5][c]
	9.29 ± 0.56	LP-LIF	[5][d]
	9.29 ± 0.77	LP-LIF	[5][e]
$CF_3CH(OH)CF_3$	2.58 ± 0.12	DF-LIF	this work
	2.65 ± 0.20	LP-LIF	this work
	2.34 ± 0.12	FP-LIF	this work

[a] DF, discharge flow; LP, laser photolysis; FP, flash photolysis; LIF, laser-induced fluorescence; RF, resonance fluorescence. [b] The quoted errors of this work and ref 4 represent 95% confidence level, and 2 σ for ref 4. [c] Measured at total pressure of 50 Torr. [d] Measured at total pressure of 75 Torr. [e] Measured at total pressure of 100 Torr.

are not considered. The systematic errors in our experiments are estimated to be less than ±10%. As is apparent in Table 1, the rate constants measured by the three different methods agree with each other within the estimated uncertainties. The literature data of the OH with CF_3CH_2OH are listed in Table 1. The present results agree with the ones in references[4,5] within the estimated uncertainties.

As was stated at the beginning of this section, gas chromatographic analysis showed that the purity for the $CF_3CF_2CH_2OH$ sample is 99.56%, which is not very good. To examine the effect of reactive impurities on the measured rate constant of OH with $CF_3CF_2CH_2OH$, the sample of $CF_3CF_2CH_2OH$ was subjected to purification process by means of a gas chromatographic method. The OH reaction rate constants for $CF_3CF_2CH_2OH$ at 298 K measured by using the original sample (99.56% purity) were $(1.10 \pm 0.06) \times 10^{-13}$, $(9.82 \pm 0.34) \times 10^{-14}$, and (1.02

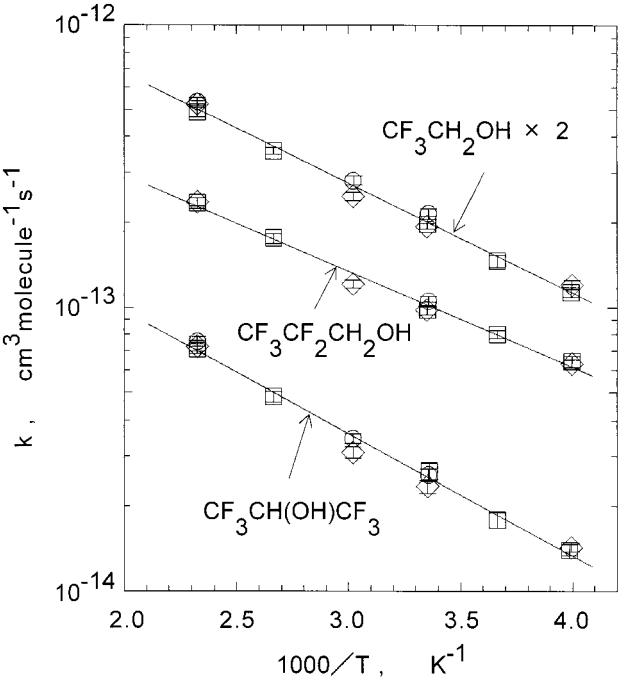

Figure 9. Arrhenius plots of the reaction rate coefficients for OH with CF_3CH_2OH, $CF_3CF_2CH_2OH$, and $CF_3CH(OH)CF_3$. The solid lines represent least-squares fit to the data. The error bars represent 95% confidence level from linear least-squares analysis. (○), DF-LIF; (□), LP-LIF; (◇), FP-LIF.

$\pm$ 0.04) $\times$ 10^{-13} cm^3 $molecule^{-1}$ s^{-1} for DF, LP, and FP methods, respectively. On the other hand, the values measured for the purified sample (99.935% purity) were (1.05 $\pm$ 0.05) $\times$ 10^{-13}, (9.78 $\pm$ 0.37) $\times$ 10^{-14}, and (9.74 $\pm$ 0.35) $\times$ 10^{-14} cm^3 $molecule^{-1}$ s^{-1} for DF, LP, and FP methods, respectively. Although the concentrations of individual impurities contained in the purified sample is about one-seventh of the original sample, the measured rate constants for the two samples with three different methods all agree with each other within the estimated uncertainties. For the purified sample of $CF_3CF_2CH_2OH$, even if the OH rate constants of impurities are as large as (1.0×10^{-11} cm^3 $molecule^{-1}$ s^{-1}), the influence of impurities on the measured rate constants may be 6.5% or less, while for the original sample the influence is estimated to be 44% at the worst case. Thus, it is concluded that the effect of impurities on the measured rate constant for purified $CF_3CF_2CH_2OH$ is negligibly small. As shown in Table 1, our results of the OH reaction rate with $CF_3CF_2CH_2OH$ agree with the ones in ref 5 within the estimated uncertainties. At lower temperatures, however, since the effect of reactive impurities on the rate constant measurement may become large if the corresponding activation energies are small, the purified sample of $CF_3CF_2CH_2OH$ was used in the further kinetic measurements.

The OH reaction rate constants of CF_3CH_2OH, $CF_3CF_2CH_2OH$, and $CF_3CH(OH)CF_3$ over the temperature range 250−430 K, measured using different methods are listed in Tables 2, 3, and 4, respectively. The experimental conditions of individual measurements are also listed in these tables. Figure 9 shows the Arrhenius plots for the OH reactions for these fluorinated alcohols. The Arrhenius plots give linear relationships in the temperature range examined. The differences among the results obtained by the three different methods are small. The Arrhenius rate parameters for the OH reactions of the fluorinated alcohols are listed in Table 5. The preexponential factors and activation energies of CF_3CH_2OH and $CF_3CF_2CH_2OH$ both have very similar values. This shows that the substitution of a CF_3 group attached to the neighboring carbon atom by C_2F_5 group is small for the OH radical rate constant.

On the other hand, a method of predicting the OH reaction rate constants has been developed by Atkinson and co-worker based on the structure activity relationship (SAR).[6−8] This method itself can be applied to a wide range of reactions such as the H-atom abstraction from C−H and O−H bonds, OH addition to double and triple bonds, OH addition to aromatic rings, and OH interaction with N-, S-, and P-containing groups. However, it has been reported that the method does not work well for the compounds such as CHF_3, CH_3CF_3, $CHF_2CF_2CF_2CF_2H$,[8] and fluorinated ethers.[9] For example, the predicted rate constants for CF_3CH_2OH at 298 K[8] is around four times larger than the present result. The cause of disagreement between the predicted and measured rate constants for fluorinated ethers can be attributed to the fact that the SAR method considers only next-neighbor atomic groups.[9] For halogenated ethers, the agreement is improved by introducing new substituent groups such as $-OCF_3$.[8] On the other hand, DeMore has proposed to consider the influence of the third group when two atoms are already attached to the C−H bond.[10] For F-, Cl-, and Br-containing C_1-C_5 alkanes, the rate constants predicted by DeMore's method agree well with the experimental data. However, the OH reaction rate constants of fluorinated alcohols such as those reported in the present paper cannot be well predicted by the existing methods.

In this paper, we have reexamined the prediction method of the H-atom abstraction rate constants from C−H and O−H bonds. The method described here is similar to the ones such as reported by Atkinson[6−8] and DeMore.[10] Here, the total reaction rate constant for the H abstraction is obtained as the sum of contributions from each C−H and/or O−H bonds present in the molecule.

$$k_{\text{total}} = \sum [k_{(\text{CH})} F(-\text{X})_\text{I} F(-\text{Y})_\text{I} F(-\text{Z})_\text{I} \text{MP}_\text{III}] + \sum [k_{(\text{CH})} F(-\text{X})_\text{I} F(-\text{Y})_\text{II} \text{MP}_\text{II}] \sum [k_{(\text{CH})} F(-\text{X})_\text{III}] + \sum [k_{(\text{OH})} F(-\text{X})_\text{I}]$$

where, $k_{(\text{CH})}$ and $k_{(\text{OH})}$ are the rate constants per C−H and O−H, and $F(-\text{X})$, $F(-\text{Y})$, and $F(-\text{Z})$ are the substituent factors for substituent groups −X, −Y, and −Z. The subscript I for substituent factor, $F(-\text{X})$ indicates that only one substituent group −X is attached to the target C−H. The subscript II and III for $F(-\text{X})$ indicate that the same two or three atoms (or atomic groups) are attached to the C−H. The multiplier, MP_II, MP_III, represent the synergistic effect when different two or three substituent groups are attached to the C−H. Here, when −F atoms and substituent groups containing fluorine atoms such as $-CF_3$, $-CH_nF_{(3-n)}$ (n = 1,2), $-CF_2-$, and −CHF− are attached to the target C−H, these numbers are considered to evaluate the multiplier. On the other hand, when −H atom, $-CH_3$, $-CH_2-$, −CH< are attached to the C−H, this number is not considered for the evaluation of the multiplier. For example, the estimated rate constant of $CF_3CHFCHF_2$ (HFC-236ea), which include two different active sites, is obtained from the following equation:

$$k = k_{(\text{CH})} F(-\text{CF}_3)_\text{I} F(-\text{F})_\text{I} F(-\text{CHF}_2)_\text{I} \text{MP}_\text{III} + k_{(\text{CH})} F(-\text{CHF}-)_\text{I} \text{F}(-\text{F})_\text{II} \text{MP}_\text{II}$$

The rate parameters, $k_{(\text{CH})}$, $k_{(\text{OH})}$, substituent factors ($F(-\text{X})$), and multipliers (MP_II, MP_III) are determined from the literature data shown in Table 6 by using a nonlinear least−squares

TABLE 2: Experimental Conditions and Results for Measurements of OH Radicals with CF_3CH_2OH[a]

temperature, (K)	method[b]	$k \times 10^{14}$ (cm^3 $molecule^{-1}$ s^{-1})	U or $\bar{t}$ range[c] (m s^{-1} or s)	pressure range, (Torr)	$[CF_3CH_2OH]$ range $\times 10^{-15}$ (molecule cm^{-3})	no. of expts
250	LP	5.66 ± 0.22	0.26−0.35	20−40	1.04−9.38	6
	FP	6.01 ± 0.23	0.32−0.41	20−40	0.82−9.11	6
273	LP	7.30 ± 0.38	0.22−0.34	20−40	0.67−9.58	6
298	DF	10.7 ± 0.5	6.6−10.6	4−5	0.15−0.91	8
	LP	9.86 ± 0.41	0.32−0.47	20−40	0.46−4.74	6
	FP	9.68 ± 0.23	0.24−0.55	10−40	0.70−9.53	6
331	DF	14.0 ± 0.5	8.0−9.9	4−5	0.16−0.93	6
	FP	12.4 ± 0.4	0.25−0.41	20−40	1.15−8.71	6
375	LP	17.8 ± 0.5	0.25−0.35	20−40	0.90−9.34	6
430	DF	26.7 ± 0.8	11.9−14.1	4−5	0.11−0.57	6
	LP	24.4 ± 1.0	0.26−0.34	20−40	0.98−9.70	6
	FP	26.1 ± 0.7	0.26−0.34	20−40	0.72−9.33	6

[a] The quoted errors represent 95% confidence level from linear least-squares analysis. [b] DF, discharge flow; LP, laser photolysis; FP, flash photolysis. [c] Linear flow velocity for DF method; $\bar{t}$, residence time for FP and LP methods.

TABLE 3: Experimental Conditions and Results for Measurements of OH Radicals with $CF_3CF_2CH_2OH$[a]

temperature, (K)	method[b]	$k \times 10^{14}$ (cm^3 $molecule^{-1}$ s^{-1})	U or $\bar{t}$ range[c] (m s^{-1} or s)	pressure range, (Torr)	$[CF_3CH_2OH]$ range $\times 10^{-15}$ (molecule cm^{-3})	no. of expts
250	LP	6.42 ± 0.27	0.29−0.51	20−40	0.54−4.92	6
	FP	6.31 ± 0.21	0.32−0.40	20−30	0.38−4.48	6
273	LP	8.01 ± 0.27	0.33−0.44	15−40	0.67−4.75	7
298	DF	10.5 ± 0.5	6.6−8.1	5	0.11−0.76	7
	LP	9.78 ± 0.37	0.25−0.33	20−30	0.56−4.77	5
	FP	9.74 ± 0.35	0.33−0.52	15−40	0.48−4.57	5
331	FP	12.1 ± 0.4	0.35−0.43	15−40	0.41−4.85	6
375	LP	17.6 ± 0.7	0.27−0.35	15−30	0.39−3.75	6
430	LP	23.4 ± 0.9	0.26−0.33	15−30	0.54−3.83	6
	FP	23.6 ± 0.7	0.24−0.33	20−30	0.29−3.82	6

[a] The quoted errors represent 95% confidence level from linear least-squares analysis. [b] DF, discharge flow; LP, laser photolysis; FP, flash photolysis. [c] U, linear flow velocity for DF method; $\bar{t}$, residence time for FP and LP methods.

TABLE 4: Experimental Conditions and Results for Measurements of OH Radicals with $CF_3CH(OH)CF_3$[a]

temperature, (K)	method[b]	$k \times 10^{14}$ (cm^3 $molecule^{-1}$ s^{-1})	U or $\bar{t}$ range[c] (m s^{-1} or s)	pressure range, (Torr)	$[CF_3CH_2OH]$ range $\times 10^{-15}$ (molecule cm^{-3})	no. of expts
250	LP	1.40 ± 0.07	0.30−0.42	20−60	0.78−9.24	7
	FP	1.43 ± 0.05	0.32−0.43	20−40	0.66−9.38	6
273	LP	1.79 ± 0.11	0.31−0.45	20−70	0.79−9.06	5
298	DF	2.58 ± 0.12	5.4−7.2	5−6	0.21−2.31	7
	LP	2.65 ± 0.20	0.32−0.42	20−60	1.24−9.20	7
	FP	2.34 ± 0.12	0.19−0.57	20−60	0.43−9.76	10
331	DF	3.45 ± 0.14	5.9−8.8	5−6	0.17−1.83	6
	FP	3.09 ± 0.14	0.25−0.39	20−40	1.29−9.15	5
375	LP	4.83 ± 0.21	0.26−0.35	20−40	0.77−9.36	7
430	DF	7.54 ± 0.29	8.4−11.2	4−6	0.19−1.45	7
	LP	7.11 ± 0.30	0.26−0.36	20−40	1.33−9.17	7
	FP	7.23 ± 0.24	0.26−0.34	20−40	0.75−9.69	6

[a] The quoted errors represent 95% confidence level from linear least-squares analysis. [b] DF, discharge flow; LP, laser photolysis; FP, flash photolysis. [c] U, linear flow velocity for DF method; $\bar{t}$, residence time for FP and LP methods.

TABLE 5: Arrhenius Rate Parameters for the Reactions of OH Radicals with CF_3CH_2OH, $CF_3CF_2CH_2OH$, and $CF_3CH(OH)CF_3$ over the Temperature Range 250−430 K[a]

fluorinated alcohol	$A \times 10^{12}$ (cm^3 $molecule^{-1}$ s^{-1})	E/R, (K)	$k_{298} \times 10^{14}$ [b] (cm^3 $molecule^{-1}$ s^{-1})	purity (%)
CF_3CH_2OH	2.00 ± 0.37	890 ± 60	10.0 ± 0.4	99.994
$CF_3CF_2CH_2OH$	1.40 ± 0.27	780 ± 60	10.2 ± 0.4	99.935
$CF_3CH(OH)CF_3$	0.699 ± 0.156	990 ± 70	2.52 ± 0.11	99.999

[a] The quoted errors represent 95% confidence level from linear least-squares analysis. [b] Rate constant at 298 K.

procedure to minimize the sum of squares of relative error between estimated (k_{est}) and experimental (k_{exp}) OH rate constants, $(k_{est} - k_{exp})/k_{exp}$. Here, all parameters except one are independent and can be determined by the least squares procedure. $F(-CH_3)$ was set equal to unity, as was done by Atkinson.[6−8]

The following three estimation methods in addition to the method described above were examined: (i) The synergistic effects of the −H atom, the $-CH_3$ group, etc., are taken into consideration together with the −F atom and the fluorine-containing groups, (ii) the substituent factors of the −H atom are not taken into consideration (assuming $F(-H)_I = F(-H)_{II} = F(-H)_{III} = 1$), and (iii) the synergistic effects of the −F atom, the $-CF_3$ group, etc., are not taken into consideration (assuming $MP_{II} = MP_{III} = 1$). As a result, it has been found that the best estimation is obtained if the first method is employed.

The optimized rate parameters, $k_{(CH)}$, $k_{(OH)}$, substituent factors, and multipliers obtained from the first method are listed in Table 7. The estimated rate constants using optimized rate parameters are shown in Table 6. The experimental data are reproduced with an average error of 14.7%. The ratio between the estimated and experimental rate constants, k_{est}/k_{exp}, have been found to range from 0.50 to 1.42. For fluorinated alcohols studied here,

TABLE 6: Comparison between Estimated and Experimental OH Rate Constants at 298 K

compound	k_{est} cm^3 molecule^{-1} s^{-1}	k_{exp} cm^3 molecule^{-1} s^{-1}	k_{est}/k_{exp}	reference
CH_4	8.30×10^{-15}	8.30×10^{-15}	1.00	[11]
C_2H_6	3.70×10^{-13}	2.70×10^{-13}	1.37	[11]
C_3H_8	7.56×10^{-13}	1.10×10^{-12}	0.69	[11]
n-C_4H_{10}	1.54×10^{-12}	2.55×10^{-12}	0.60	[6]
i-C_4H_{10}	2.37×10^{-12}	2.37×10^{-12}	1.00	[6]
CH_3OH	8.05×10^{-13}	9.00×10^{-13}	0.89	[11]
C_2H_5OH	3.75×10^{-12}	3.40×10^{-12}	1.10	[11]
n-C_3H_7OH	3.24×10^{-12}	5.30×10^{-12}	0.61	[11]
i-C_3H_7OH	6.32×10^{-12}	5.60×10^{-12}	1.13	[11]
CF_3CH_2OH	1.00×10^{-13}	1.00×10^{-13}	1.00	this work
$CF_3CF_2CH_2OH$	1.04×10^{-13}	1.02×10^{-13}	1.02	this work
$CF_3CH(OH)CF_3$	2.51×10^{-14}	2.52×10^{-14}	1.00	this work
CHF_3 (23)	2.74×10^{-16}	2.74×10^{-16} [a]	1.00	[12, 13]
CH_2F_2 (32)	1.00×10^{-14}	1.06×10^{-14} [a]	0.94	[12, 14]
CH_3F (41)	1.64×10^{-14}	1.97×10^{-14} [a]	0.83	[10, 13]
CHF_2CF_3 (125)	1.93×10^{-15}	1.90×10^{-15}	1.01	[14]
CHF_2CHF_2 (134)	5.14×10^{-15}	5.70×10^{-15}	0.90	[15
CH_2FCF_3 (134a)	4.91×10^{-15}	4.07×10^{-15} [a]	1.21	[15, 16]
CH_2FCHF_2 (143)	2.08×10^{-14}	1.67×10^{-14} [a]	1.24	[17, 18]
CH_3CF_3 (143a)	1.07×10^{-15}	1.30×10^{-15} [a]	0.82	[12, 14, 19]
CH_2FCH_2F (152)	7.25×10^{-14}	1.12×10^{-13}	0.65	[18]
CH_3CHF_2 (152a)	3.47×10^{-14}	3.57×10^{-14} [a]	0.97	[12, 16, 20]
CH_3CH_2F (161)	9.28×10^{-14}	1.84×10^{-13} [a]	0.50	[12, 13]
CF_3CHFCF_3 (227ea)	1.18×10^{-15}	1.61×10^{-15} [a]	0.73	[12, 21]
$CF_3CHFCHF_2$ (236ea)	5.02×10^{-15}	5.20×10^{-15} [a]	0.97	[12, 22]
$CF_3CH_2CF_3$ (236fa)	3.97×10^{-16}	3.40×10^{-16}	1.17	[12]
$CH_2FCF_2CHF_2$ (245ca)	8.15×10^{-15}	9.20×10^{-15} [a]	0.89	[12, 21]
$CHF_2CHFCHF_2$ (245ea)	1.60×10^{-14}	1.60×10^{-14}	1.00	[22]
CF_3CHFCH_2F (245eb)	1.57×10^{-14}	1.48×10^{-14}	1.06	[22]
$CHF_2CF_2CF_2CF_2H$ (338pcc)	4.59×10^{-15}	4.58×10^{-15} [a]	1.00	[13, 23]
$CF_3CH_2CH_2CF_3$ (356ffa)	7.45×10^{-15}	8.75×10^{-15}	0.85	[21]
$CF_3CF_2CH_2CH_2F$ (356mcf)	6.01×10^{-14}	4.22×10^{-14}	1.42	[22]
$CF_3CHFCHFCF_2CF_3$ (43−10mee)	3.37×10^{-15}	3.43×10^{-15} [a]	0.98	[13, 23]
$CF_3CF_2CH_2CH_2CF_2CF_3$ (55−10mcff)	8.88×10^{-15}	8.30×10^{-15}	1.07	[22]

[a] Averaged value of references.

TABLE 7: Derived Contribution Factors for OH Rate Constant Estimations

parameter	value
$k_{(CH)}$	3.18×10^{-12} [a]
$k_{(OH)}$	1.18×10^{-13} [a]
$F(-H)_I$	0.150
$F(-H)_{II}$	0.0194
$F(-H)_{III}$	0.000653
$F(-CH_3)_I$	1.00 [b]
$F(-CH_3)_{II}$	0.529
$F(-CH_3)_{III}$	0.715
$F(-CH_2-)_I$	0.675
$F(-CH<)_I$	0.171
$F(-OH)_I$	3.71
$F(-F)_I$	0.0888
$F(-F)_{II}$	0.0105
$F(-F)_{III}$	0.0000862
$F(-CF_3)_I$	0.00577
$F(-CF_3)_{II}$	0.000416
$F(-CHF_2)_I$	0.00771
$F(-CHF_2)_{II}$	0.00280
$F(-CH_2F)_I$	0.0426
$F(-CF_2-)_I$	0.00688
$F(-CHF-)_I$	0.0121
MP_{II}	10.0
MP_{III}	78.1

[a] Units are cm^3 molecule^{-1} s^{-1}. [b] By definition.

the estimated rate constants reproduce the experimental values within a factor of 1.00 to 1.02.

Inspection of Table 7 reveals some general features of the substitution effects. The fact that the substituent factors of $-CH_3$ and $-CH_2-$ are close to unity indicates that these substituent groups increase the reactivity of C−H compared with others.

TABLE 8: The Synergistic Effect of the Substituent Factor *F*(−X)

$F(-X)$	$F(-X)_I$	$F(-X)_{II}$	$F(-X)_{II}/F(-X)_I^2$	$F(-X)_{III}$	$F(-X)_{III}/F(-X)_I^3$
$F(-H)$	0.151	0.0194	0.859	0.000653	0.192
$F(-F)$	0.0888	0.0105	1.33	0.0000862	0.123
$F(-CH_3)$	1.00[a]	0.529	0.529	0.715	0.715
$F(-CF_3)$	0.00577	0.000416	12.5		
$F(-CHF_2-)$	0.00771	0.00280	47.1		

[a] By definition.

The −OH group of alcohol remarkably increases the C−H reactivity. The substituent factors for the −F atom and fluorine-containing groups are smaller than ones for the −H atom and $-CH_3$ indicating that they decrease the reactivity of the C−H group when substituted for −H atom or $-CH_3$. In particular, the $-CF_3$ group most diminishes the C−H reactivity. The substituent factor of $-CF_2-$ is almost equivalent to that of $-CF_3$. In fact, there is no significant difference between the reactivities of CF_3CH_2OH and $CF_3CF_2CH_2OH$. For $-CHF_2$, $-CH_2F$, and −CHF−, the C−H reactivity is decreased with increase of the number of F atom. The multipliers for the synergistic effect between different substituent groups (MP_{II} and MP_{III}) are larger than unity, and MP_{III} is larger than MP_{II}. Thus, when two or three different substituent groups are attached to C−H, the degree of the decrease in the C−H reactivity by individual substituent groups becomes small.

The synergistic effects of substituent factor, $F(-X)$, are summarized in Table 8. The substituent factors, $F(-H)_{III}$, $F(-F)_{III}$, $F(-CH_3)_{III}$, and $F(-CHF_2)_{II}$, are determined by using the data of CH_4, CHF_3, *i*-C_4H_{10}, and $CHF_2CHFCHF_2$ (HFC-245ea), respectively, and are irrespective of other compounds. Since

$F(-CF_3)_{II}/F(-CF_3)_I^2$ is larger than unity, the degree of decreasing the C−H reactivity per one $-CF_3$ decreases if two $-CF_3$ groups are attached together to the C−H. A similar tendency is also noted for the relationship between $F(-F)_I$ and $F(-F)_{II}$, and that between $F(-CHF_2)_I$ and $F(-CHF_2)_{II}$. This is in accord with the fact that the corresponding multipliers are larger than unity. As for $F(-F)_I$, $F(-F)_{II}$, and $F(-F)_{III}$, $F(-F)_{III}$ is by far smaller than the others. It seems that the reactivity of OH with CHF_3 cannot be explained in line with other molecules. A similar tendency is also recognized in the relations among $F(-H)_I$, $F(-H)_{II}$, and $F(-H)_{III}$.

In this report, the synergistic effects due to multiple substituent groups (MP_{II} and MP_{III}) were obtained irrespective of the magnitude of individual substituent factors. However, as is seen in Table 8, the synergistic effect of substituent groups seems to depend on the magnitude of substituent factors. Thus, it seems necessary to consider the following items in order to obtain the estimated rate constants for a wider range of compounds with enough accuracy. First, the synergistic effect between different substituent groups may depend on the magnitude of individual substituent factors. Therefore, the improvement of the accuracy of estimation can be expected by considering the magnitude of individual substitution effects to synergistic effect between the substituent groups. Second, it is necessary to consider the method of obtaining the substituent factors from individual constituent atoms, though in this work the substituent factors were treated for groups in such cases as $-CH_3$ and $-CF_3$. This means, however, that the long-range effects of substitution are taken into consideration. As a result, it may become possible to estimate the rate constants of such molecules as ethers with sufficient accuracy.

Finally, the temperature dependency of the reaction rate constants was not examined in the present study. However, as has been done by Atkinson et al., the temperature dependency of the rate constants may be reproduced by applying Arrhenius's expression to $k_{(CH)}$ and $k_{(OH)}$, and $\exp(E_X/T)$ to the substituent factor $F(-X)$.

Acknowledgment. The present investigation has been performed with the support of the New Energy and Industrial Technology Development Organization.

References and Notes

(1) "Scientific Assessment of Ozone Depletion: 1994", UNEP/WMO, Global Ozone Research and Monitoring Project − Report No.37.

(2) Burrows, J. P.; Wallington, T. J.; Wayne, R. P. *J. Chem. Soc., Faraday Trans. 2* **1983**, *79*, 111.

(3) Kaufman, F. *J. Prog. React. Kinet.* **1961**, *1*, 1.

(4) Wallington, T. J.; Dagaut, P.; Kurylo, M. J. *J. Phys. Chem.* **1988**, *92*, 5024.

(5) Inoue, G.; Izumi, K.; Lozovsky. V. A. Third International Conference on Chemical Kinetics, Gaithersburg, MD, 1993; pp 182−183.

(6) Atkinson, R. *Chem. Rev.* **1986**, *86*, 69.

(7) Atkinson, R. *Int. J. Chem. Kinet.* **1987**, *19*, 799.

(8) Kwok, E. S. C.; Atkinson, R. *Atmos. Environ.* **1995**, *29*, 1685.

(9) Zhang, Z.; Saini, R. D.; Kurylo, M. J.; Huie, R. E. *J. Phys. Chem.* **1992**, *96*, 9301.

(10) DeMore, W. B. *J. Phys. Chem.* **1996**, *100*, 5813.

(11) Atkinson, R.; Baulch, D. L.; Cox, R. A.; Hampspn, R. F., Jr.; Kerr, J. A.; Troe, J. *J. Phys. Chem. Ref. Data* **1989**, *18*, 881.

(12) Hsu, K. J.; DeMore, W. B. *J. Phys. Chem.* **1995**, *99*, 1235.

(13) Schmoltner, A. M.; Talukdar, R. K.; Warren, R. F.; Mellouki, A.; Goldfarb, L.; Gierczak, T.; McKeen, S. A.; Ravishankara, A. R. *J. Phys. Chem.* **1993**, *97*, 8976.

(14) Talukdar, R. K.; Mellouki, A.; Gierczak, T.; Burkholder, J. B.; McKeen, S. A.; Ravishankara, A. R. *J. Phys. Chem.* **1991**, *95*, 5815.

(15) DeMore, W. B. *Geophys. Res. Lett.* **1993**, *20*, 1359.

(16) Gierczak, T.; Talukdar, R. K.; Vaghjiani, L. V.; Lovejoy, E. R.; Ravishankara, A. R. *J. Geophy. Res.* **1991**, *96*, 5001.

(17) Barry, J.; Sidebottom, H.; Treacy, J.; Franklin, J. *Int. J. Chem. Kinet.* **1995**, *27*, 27.

(18) Martin, J.-P.; Paraskevopoulos, G. *Can. J. Chem.* **1983**, *61*, 861.

(19) Orkin, V. L.; Huie, R. E.; Kurylo, M. J. *J. Phys. Chem.* **1996**, *100*, 8907.

(20) Liu, R.; Huie, R. E.; Kurylo, M. J. *J. Phys. Chem.* **1990**, *94*, 3247.

(21) Zhang, Z.; Padmaja, S.; Saini, R. D.; Huie, R. E.; Kurylo, M. J. *J. Phys. Chem.* **1994**, *98*, 4312.

(22) Nelson, D. D., Jr.; Zahniser, M. S.; Kolb, C. E.; Magid, H. *J. Phys. Chem.* **1995**, *99*, 16301.

(23) Zhang, Z.; Kurylo, M. J.; Huie, R. E. *Chem. Phys. Lett.* **1992**, *200*, 230.